



AALBORG UNIVERSITY
DENMARK

Aalborg Universitet

Papers

Volume 6: 2001-2003

Thoft-Christensen, Palle

Publication date:
2007

Document Version
Publisher's PDF, also known as Version of record

[Link to publication from Aalborg University](#)

Citation for published version (APA):
Thoft-Christensen, P. (2007). *Papers: Volume 6: 2001-2003*. Department of Civil Engineering, Aalborg University.

General rights

Copyright and moral rights for the publications made accessible in the public portal are retained by the authors and/or other copyright owners and it is a condition of accessing publications that users recognise and abide by the legal requirements associated with these rights.

- Users may download and print one copy of any publication from the public portal for the purpose of private study or research.
- You may not further distribute the material or use it for any profit-making activity or commercial gain
- You may freely distribute the URL identifying the publication in the public portal -

Take down policy

If you believe that this document breaches copyright please contact us at vbn@aub.aau.dk providing details, and we will remove access to the work immediately and investigate your claim.

CHAPTER 113

IMPROVING THE DYNAMICS OF SUSPENSION BRIDGES USING ACTIVE CONTROL SYSTEMS¹

P. Thoft-Christensen

Aalborg University, Aalborg, Denmark

ABSTRACT

Improving the dynamics of suspension bridge using active control is discussed in this paper. The main dynamic problem with long suspension bridges is the aeroelastic phenomenon called flutter. Flutter oscillations of a bridge girder is a stability problem and the oscillations are perpendicular to the direction of the wind and occur when the bridge is exposed to wind velocity above a critical value called the flutter wind velocity U_{cr} . U_{cr} decreases with decreasing stiffness and damping. Flutter is therefore a serious problem for bridges with a relatively low stiffness such as long bridges. Installation of passive and active control devices may be a solution to the girder stability problem. In the literature a number of such devices have been discussed, e.g. viscoelastic damping elements, tuned damping elements, and eccentric masses. In this paper an active control system based on movable flaps attached to the bridge girder is presented. Tunnel experiments with a bridge section show that flaps are effective in controlling the flutter of bridge girders.

1. INTRODUCTION

Several short span (< 500 m) bridges collapsed due to the wind; see figure 1. The famous and relatively long (854 m) Tacoma Narrows Bridge failed in 1940; see figure 2. In recent years much longer bridges have been constructed. The longest suspension bridge today is the Akashi Kaikyo Bridge in Japan (main span 1991 m) and the second longest is the Great Belt East Bridge in Denmark (main span 1624 m); see figure 3.

¹ 2nd International Workshop on “Life-Cycle Cost Analysis and Design of Civil Infrastructure Systems”, Ube Yamaguchi, Japan, September 27-29, 2001. In the Proceedings “Maintaining the Safety of Deteriorating Civil Infrastructures”, pp. 293-304.

Bridge	Location	Year	Main Span [m]	WIDTH of Deck [m]	Designer
1. Dryburgh Abbey	Scotland	1818	79	1.2	John & W. Smith
2. Nassau	Germany	1834	75	-	Lossen & Wolf
3. Brighton Chain Pier	England	1836	78	3.9	Samuel Brown
4. Montrose	Scotland	1838	132	7.9	Samuel Brown
5. Menai Straits	Wales	1839	177	7.3	Thomas Telford
6. Roche-Bernard	Scotland	1852	79	1.2	John & W. Smith
7. Wheeling	U.S.A.	1854	309	7.3	Charles Ellet
8. Lewiston-Queenston	U.S.A.	1864	318	5.9	Edward Serrell
9. Niagara-Clifton	U.S.A.	1889	386	5.2	Samuel Keefer
10. Tacoma Narrows	U.S.A.	1940	854	11.9	Leon Moisseiff

Figure 1. Suspension bridge failures (taken from Hyunh [1]).

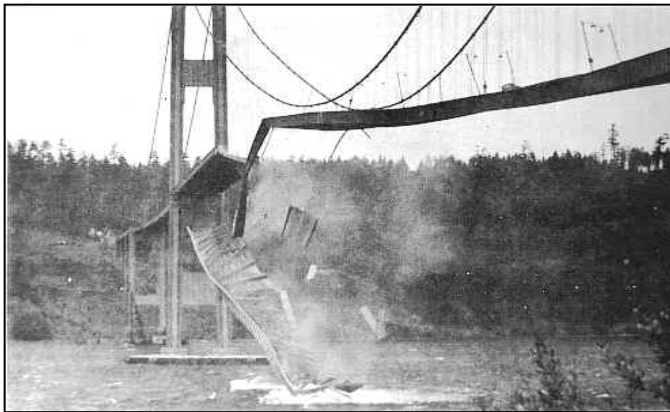


Figure 2. Failure of the Tacoma Narrows Bridge in 1940 (taken from Hyunh [1]).

Future designs with improved girder forms, lightweight cables, and control devices may be up to 3000-5000 m long. For such extremely long bridges, girder stability to wind action may be a serious problem, especially when the girder depth-to-width ratio is small compared with existing long bridges.



Figure 3. Great Belt East Bridge, Denmark (taken from Huynh [1]).

2. FLUTTER CONTROL

In this paper a brief overview of research work done in Denmark on the application of flaps to active control of flutter of long suspension bridges is given. Ostenfeld and Larsen [2] proposed in 1992 to ensure the aerodynamic stability of slender bridge girders by attaching actively controlled flaps along the girders. The effect of these flaps is that they exert forces on the bridge girder when the flaps are exposed to wind. The

rotation of the flaps is controlled in such a way that these forces counteract the aerodynamic forces and therefore damp the oscillations. At Aalborg University two topics within this area have been investigated in recent years, see the Ph.D. thesis by Hansen [3] and Huynh [1]. The results of these studies are published in several papers e.g. by Hansen & Thoft-Christensen [4], [5], [6], [7], Hansen, Thoft-Christensen, Mendes & Branco [8], Huynh & Thoft-Christensen [9], [10], Thoft-Christensen [11]. The present paper is strongly based on references [1] to [11].

The thesis by Hansen [3] deals with wind tunnel experiments with a sectional model of a girder where the control flaps are installed as integrated parts of the leading and trailing edges of the girder. The experiments confirm that the flap control system is an efficient way to limit the girder vibrations. The experiments also confirmed that a good estimate of the flutter wind velocity for a section with flaps can be obtained simply by replacing the aerodynamic derivatives by expressions including the parameters describing the flap configuration. Also the theoretical effect of the flaps is confirmed by the experiments. Further, it can be concluded that the trailing flap is more efficient than the leading flap. Finally, moving both flaps is more efficient than using only the trailing flap.

An analysis of a full span suspension bridge is performed in the thesis by Huynh [1]. Separate control flaps are installed at the front of and under the leading and the trailing edges of the girder. The analysis shows that the effect of flaps on the girder vibrations depends on the following factors: the total sectional length of the flaps, the rotational directions, and the rotational magnitudes of the flaps. The analysis is based on data from the girder used in the Great Belt Bridge. For the used configuration of the flaps it is shown that the flutter wind velocity U_{cr} can be increased by 50% compared with a girder with no flaps. Not only the flutter response can be limited by the flap rotations, but also the buffeting response can be reduced in the mean square value. The flap rotations in turbulence conditions will change the angle of attack of the wind to the flaps so that the total buffeting induced forces acting on the girder system are reduced. The stochastic buffeting responses can be derived by a conventional stochastic response analysis in modal coordinates, and in accordance with the wind load consisting of a stochastic buffeting term and an aeroelastic term.

Controlling the vibrations of civil engineering structures using active control systems has been used primarily to fulfill serviceability and comfort requirements. For such cases failure of the control system is not critical for the users of the structures or the structure itself. The situation is completely different with regard to controlling the safety of a long-span bridge using a control system. In such a case a passive control system is preferred.

3. WIND LOADS ON A SUSPENSION BRIDGE WITHOUT FLAPS

The three most serious vibrations of a suspension bridge girder are

- Motion-induced vibrations
- Buffeting-induced vibrations and
- Vortex-induced vibrations.

The motion-induced wind loads (aeroelastic forces) depend directly on deformations and deformation velocities of the girder, see figure 4. The buffeting-induced wind loads are the fluctuating wind loads due to the turbulence of the wind.

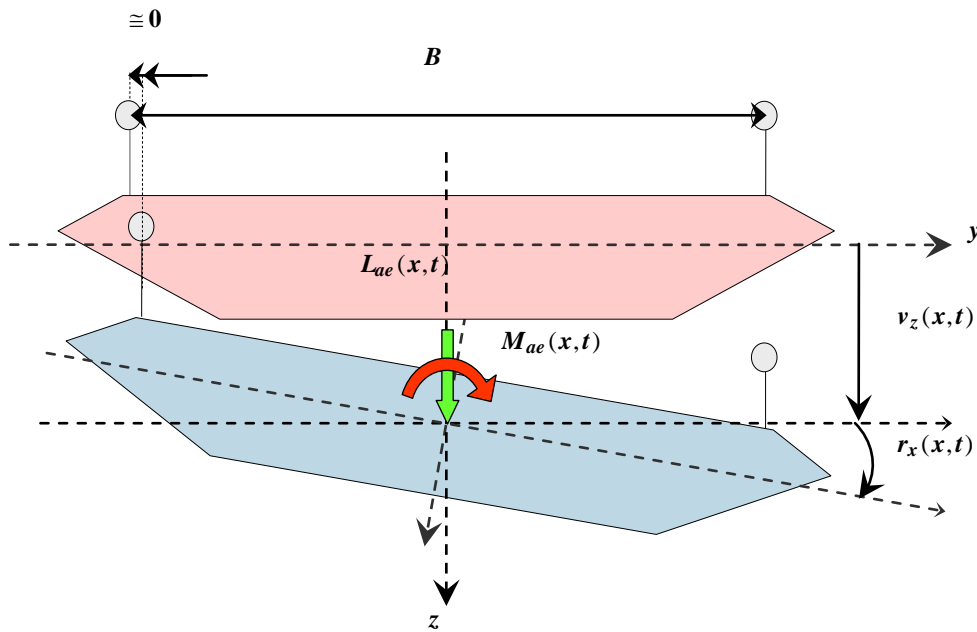


Figure 4. Motion-induced wind loads for a bridge without flaps.

By assuming potential flow theory, Theodorsen [12] has shown for thin airfoils in incompressible flow that the motion-induced vertical load $L_{ae}(x,t)$ and the motion-induced moment $M_{ae}(x,t)$ on the airfoil are linear in the theoretical displacement and the torsional angle and their first and second derivatives (see figure 4), where x is the coordinate in the direction of the bridge and t the time. Let y and z be the coordinates in the direction across the bridge and in the vertical direction. Scanlan and Tomko [13] introduced a similar formulation for bridges. The aeroelastic forces L^{deck} and M^{deck} per unit span and for small rotations can then be written, see Simulu & Scanlan [14]

$$L_{ae}^{deck}(x,t) = \frac{\rho U^2 B}{2} \left[KH_1^*(K) \frac{\dot{v}_z}{U} + KH_2^*(K) \frac{B \dot{r}_x}{U} + K^2 H_3^*(K) r_x + K^2 H_4^*(K) \frac{v_z}{B} \right] \quad (1)$$

$$M_{ae}^{deck}(x,t) = \frac{\rho U^2 B^2}{2} \left[KA_1^*(K) \frac{\dot{v}_z}{U} + KA_2^*(K) \frac{B \dot{r}_x}{U} + K^2 A_3^*(K) r_x + K^2 A_4^*(K) \frac{v_z}{B} \right] \quad (2)$$

where $K=B\omega/U$ is the non-dimensional reduced frequency, B is the girder width, U is the mean wind velocity, ω is the bridge oscillating frequency (rad.) at the wind velocity U , and ρ is air density. $H_i^*(K)$ and $A_i^*(K)$ ($i=1,2,3,4$) are non-dimensional aerodynamic derivatives which can be estimated by wind tunnel experiments. The quantities r_x , \dot{v}_z/U and $B \dot{r}_x/U$ are non-dimensional, effective angles of attack.

4. BRIDGE GIRDERS WITH FLAPS

Two types of actively controlled flaps are shown in figure 5:

- Flaps arranged on pylons below the streamlined bridge girder (the second thesis) and
- Flaps integrated in the bridge girder so each flap is the streamlined part of the edge of the girder (the first thesis).

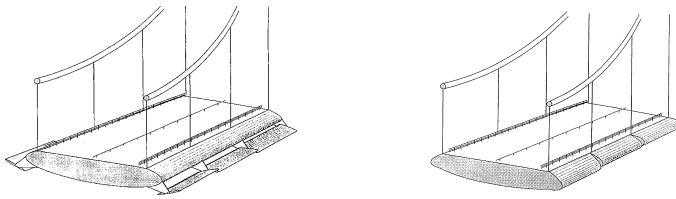


Figure 5: Sections with flaps on pylons and integrated in the section.

When the flaps are exposed to the wind they exert forces on the bridge girder. By regulating the flaps the directions and sizes of the forces may be controlled. By providing forces, which counteract the motion of the girder the oscillations are

damped. A number of sensors are placed inside the bridge girder to measure the position or motion of the girder. The measurements are transmitted to the control unit,

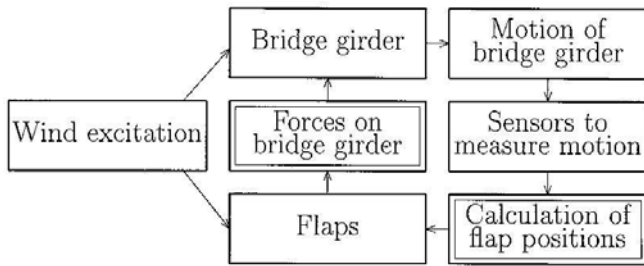


Figure 6: Active Control System.

e.g. a computer. The flaps are then regulated based on a control algorithm that uses these measurements as input. In this way the flaps can be regulated continuously to counteract the motion of the girder. The active control system is shown in figure 6.

5. WIND LOADS ON A SUSPENSION BRIDGES WITH FLAPS

In the same way as for the airfoils, the loads due to movement of a trailing flap on a thin airfoil in incompressible flow are linear in the angle of the trailing flap and in the first and second derivatives. By assuming that the angle of a leading flap has no effect on the air circulation it can be shown that the loads due to movement of a leading flap on a thin airfoil are also linear in the angle of the leading flap and in the first and second derivatives. The motion-induced wind loads due to movement of the flaps can therefore be described by additional aerodynamic derivatives.

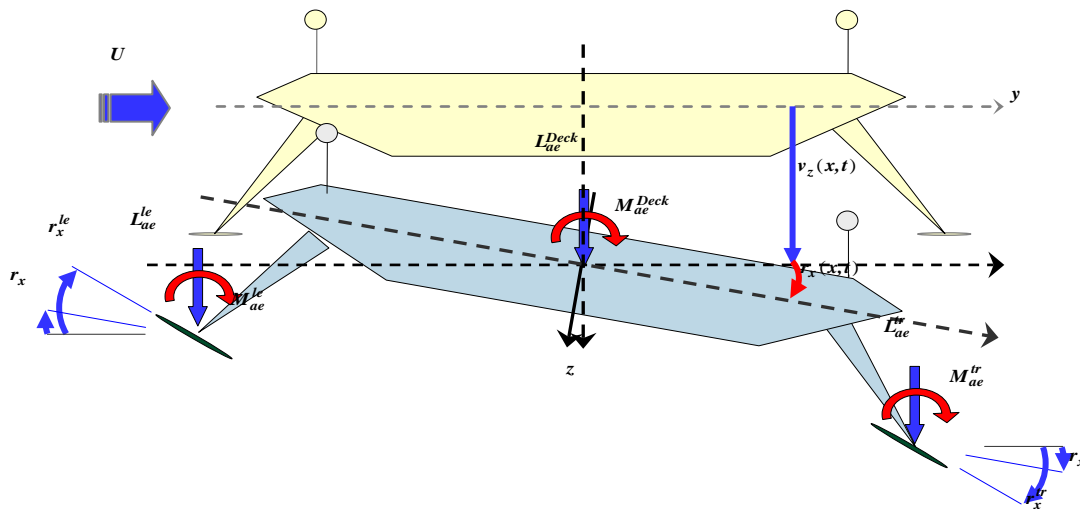


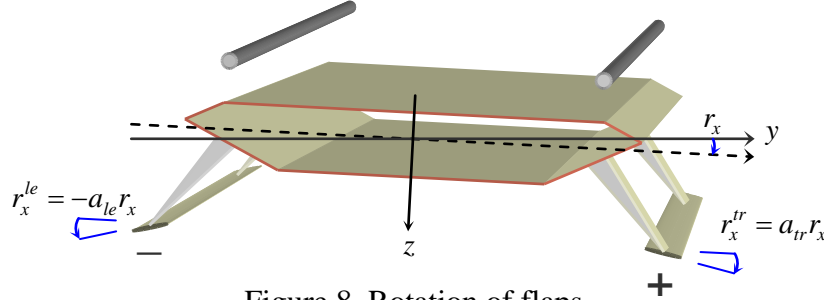
Figure 7: Motion-induced wind loads on the girder and on the flaps.

The total motion-induced wind loads per unit span on the girder and the flaps are, see figure 7,

$$L_z^{total} = L_z^{deck} + L_z^{tr}(v_z, r_x^{tr}) + L_z^{le}(v_z, r_x^{le}) \tag{3}$$

$$M_x^{total} = M_x^{Deck} + M_x^{tr}(v_z, r_x^{tr}) + M_x^{le}(v_z, r_x^{le}) + \left(L_z^{tr}(v, r_x^{tr}) - L_z^{le}(-v, r_x^{le}) \right) \frac{B}{2} \tag{4}$$

where $v_z(x,t)$ and $r_x(x,t)$ are the vertical motion and the rotation of the girder at position x along the bridge girder at the time t .



$r_x^{le}(x,t)$ and $r_x^{tr}(x,t)$ are the rotations of the leading and the trailing flaps as defined in figure 8.

Figure 8. Rotation of flaps.

6. THE THEOREICAL EFFECT OF FLAPS

Figure 9 shows the calculated flutter velocity U_{cr} for different combinations of flap rotations. α is the rotation of the girder, α_l and α_t are the rotations of the leading and the trailing flaps, φ_l and φ_t are the phase angles between the leading flap, the trailing flap and the girder, respectively. The calculations show that the flutter wind velocity U_{cr} is increased when the phase angle for the leading flap φ_l is in the interval $[0.6\pi/6; 6.6\pi/6]$, otherwise the flutter wind velocity U_{cr} is reduced. The flutter wind velocity U_{cr} for binary flutter is calculated for different values of amplification factor a_t and φ_t for the trailing flap. The calculations also show that the interval, where the flutter wind velocity is increased when the trailing flap is moved, is dependent on the flap a_t . The flutter wind velocity is generally reduced when the phase angle of the trailing flap φ_t is in the interval $[\pi/6; 6\pi/6]$. For phase angles outside this interval the flutter wind velocity is generally increased. The trailing flap is much more efficient than the leading flap.

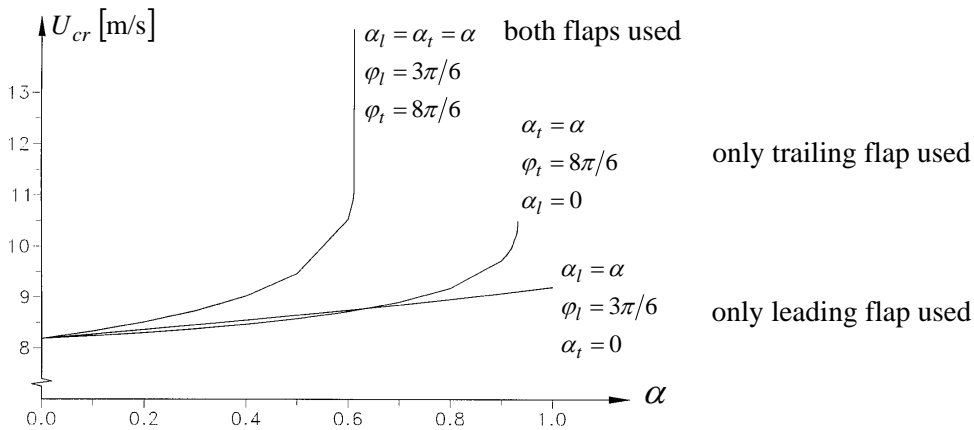


Figure 9: The theoretical effect on the flutter wind velocity of using flaps.

7. WIND TUNNEL TESTS

Wind tunnel testing of a bridge section model has been performed in a wind tunnel at Instituto Superior Técnico in Lisbon, Portugal. The bridge section model is shown in figure 10. The regulation system for moving the flaps consists of three parts: a servosystem,

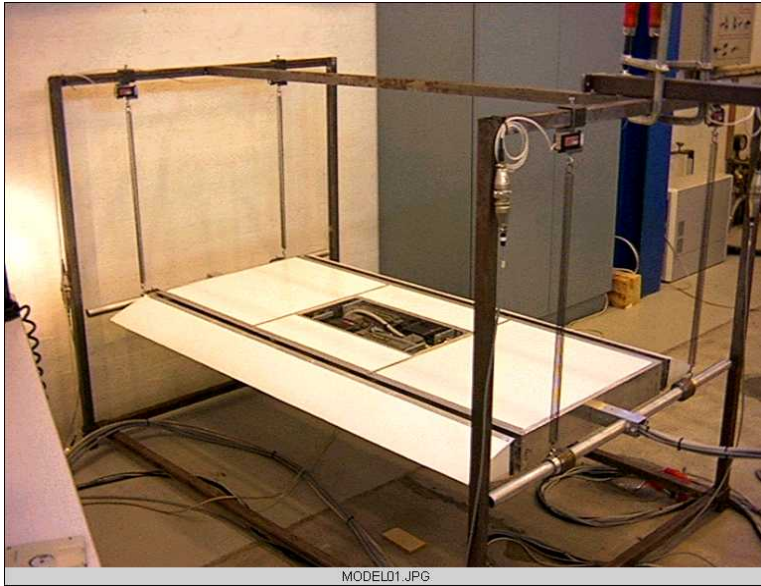


Figure 10: Wind tunnel model.

the regulation software to position the flaps, and the control software used to calculate the desired positions of the flaps. The servosystem consists of a servo-amplifier, a servomotor and a reduction gear. Two servosystems are used so that the two flaps can be regulated independently. The reduction gears and the servomotors are fixed inside the bridge section model. Each reduction gear is connected to the flaps via cables. Each servomotor is connected to a servo amplifier, which is placed outside the model. The servomotor and the gear installation are shown in figure 11.



Figure 11. Servomotor and gear installation.

Several configurations of the flaps have been tested. As seen in figure 12, the experimental damping ratio is smaller for flap configurations 0 and 1 than the theoretical damping ratio, but the shape of the curve is almost the same. For flap configuration 2 the experimental damping ratio exceeds the theoretical one. For flap configurations 1 and 2, the theoretical curves show that no binary flutter will occur.

Several configurations of the flaps have been tested. As seen in figure 12, the experimental damping ratio is smaller for flap configurations 0 and 1 than the theoretical damping ratio, but the shape of the curve is almost the same. For flap configuration 2 the experimental damping ratio exceeds the theoretical one. For flap configurations 1 and 2, the theoretical curves show that no binary flutter will occur.

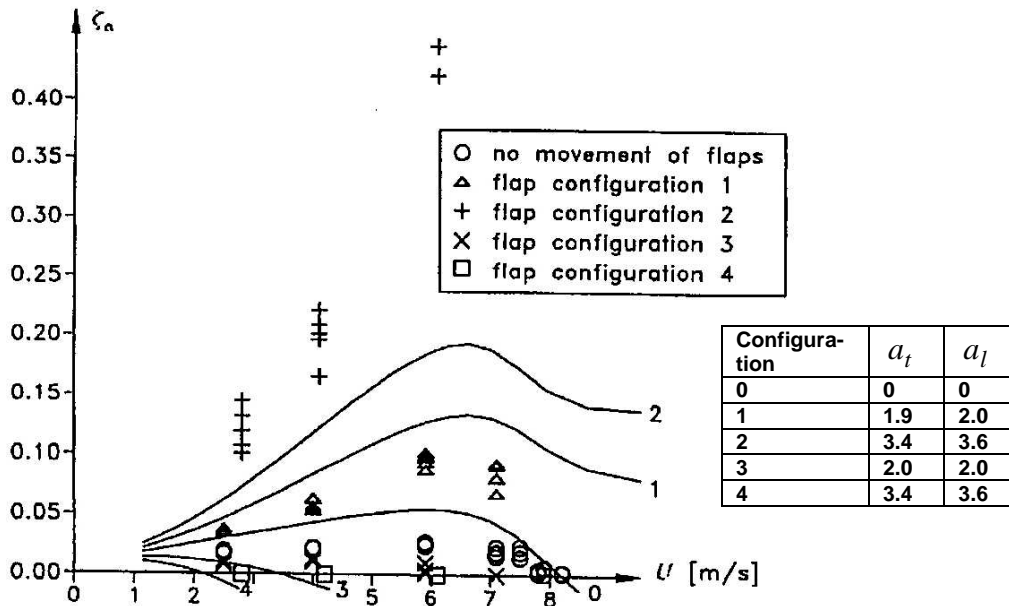


Figure 12: Theoretical (solid lines) and experimental damping ratio for torsional motion with wind for flap configurations 0-4. The number at the end of a solid line denotes the actual flap configuration.

Figures 13 and 14 show the torsional movement of the model when the flaps are not regulated (configuration 0) and when they are regulated (configuration 2). The wind speed is 6.1 m/s. Note that the units on the x-axis are different in the two figures. The conclusion is that configuration 2 is very efficient for controlling the torsional motion of the model. During the first second the torsional motion is reduced from 2.7° to 1.1°, i.e. by 62%.

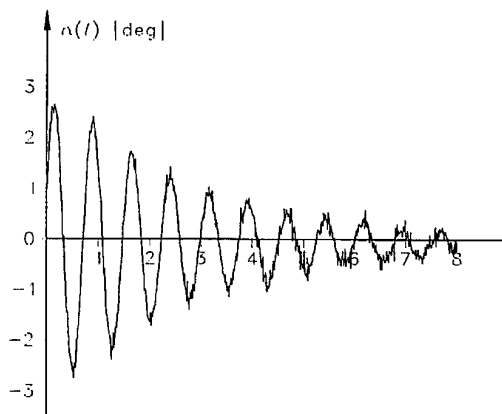


Figure 13: Torsional motion for flap configuration 0 and wind speed 6.1 m/s.

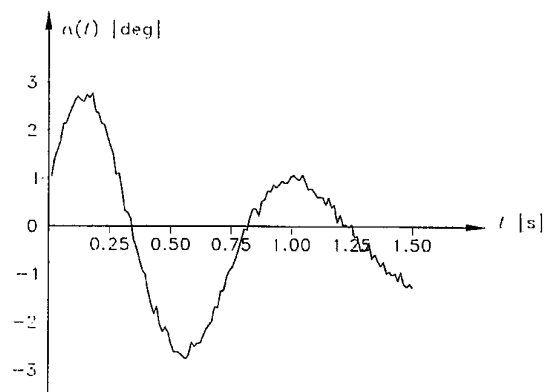


Figure 14: Torsional motion for flap configuration 2 and wind speed 6.1 m/s.

8. FLUTTER CONDITIONS

Let $\phi_i(x)$ and $\psi_j(x)$ be the vertical and the torsional mode shapes of the bridge in mode i and mode j which are assumed to be coupled at flutter. The governing modal equations for the two-mode flutter conditions are then

$$M_z \left(\ddot{z}(t) + 2\omega_z \zeta_z \dot{z}(t) + \omega_z^2 z(t) \right) = F_z^{tot}(t) \quad (5)$$

$$M_x \left(\ddot{\alpha}(t) + 2\omega_\alpha \zeta_\alpha \dot{\alpha}(t) + \omega_\alpha^2 \alpha(t) \right) = F_x^{tot}(t) \quad (6)$$

where $z(t)$ and $\alpha(t)$ are the vertical and the torsional modal coordinates. ω_z , ζ_z and ω_α and ζ_α are the natural frequencies and the damping ratios of the vertical and torsional modes. M_z and M_x are the vertical and the torsional modal masses. At the coupled motion, the vertical and the torsional modal responses are both assumed to be proportional to $e^{i\omega t}$, when the critical wind velocity is acting on the bridge, i.e. $z(t) = z_0 e^{i\omega t}$ and $\alpha(t) = \alpha_0 e^{i\omega t}$. When this is introduced into the above equations the following matrix equation can be derived

$$\mathbf{A} \begin{bmatrix} z/B \\ \alpha \end{bmatrix} = \begin{bmatrix} 0 \\ 0 \end{bmatrix} \quad (7)$$

where the system matrix \mathbf{A} depends on the natural mode shapes and frequencies, the damping ratios, the derivatives and the wind velocity. This matrix equation has non-trivial solutions when

$$\text{Det}(\mathbf{A}) = \text{Re Det}(\mathbf{A}) + i \text{Im Det}(\mathbf{A}) = 0 \quad (8)$$

resulting in the following two flutter conditions for a bridge with separate flaps, Huynh [1]:

$$\begin{aligned} \text{Re}(\text{Det}) = & \frac{\omega^4}{\omega_z^4} \left(1 + \frac{M3}{J\omega^2\Psi} + \frac{L4}{m\omega^2\Phi} + \frac{1}{mJ\omega^4\Psi\Phi} \left[-\omega^2 L1M2 + L4M3 - M4L3 + \omega^2 M1L2 \right] \right) \\ & + \frac{\omega^3}{\omega_z^3} \left(2\zeta_z \frac{M2}{J\omega\Psi} + 2\zeta_\alpha \frac{\omega_\alpha}{\omega_z} \frac{L1}{m\omega\Phi} \right) \\ & + \frac{\omega^2}{\omega_z^2} \left(-1 - \frac{\omega_\alpha^2}{\omega_z^2} - 4 \frac{\omega_\alpha}{\omega_z} \zeta_z \zeta_\alpha - \frac{M3}{J\omega^2\Psi} - \frac{\omega_\alpha^2}{\omega_z^2} \frac{L4}{m\omega^2\Phi} \right) + \frac{\omega_\alpha^2}{\omega_z^2} = 0 \end{aligned} \quad (9)$$

$$\begin{aligned} \text{Im}(\text{Det}) = & \frac{\omega^3}{\omega_z^3} \left(\frac{M2}{J\omega\Psi} + \frac{L1}{m\omega\Phi} + \frac{1}{m\omega^3\Phi J\Psi} \left[L1M3 + L4M2 - M1L3 - M4L2 \right] \right) \\ & + \frac{\omega^2}{\omega_z^2} \left(-2\zeta_z - 2\zeta_\alpha \frac{\omega_\alpha}{\omega_z} - 2\zeta_\alpha \frac{\omega_\alpha}{\omega_z} \frac{L4}{m\omega^2\Phi} - 2\zeta_z \frac{M3}{J\omega^2\Psi} \right) \\ & + \frac{\omega}{\omega_z} \left(-\frac{M2}{J\omega\Psi} - \frac{\omega_\alpha^2}{\omega_z^2} \frac{L1}{m\omega\Phi} \right) + 2\zeta_z \frac{\omega_\alpha^2}{\omega_z^2} + 2\zeta_\alpha \frac{\omega_\alpha}{\omega_z} = 0 \end{aligned} \quad (10)$$

where m is the girder mass per unit span. Φ , Ξ and Ψ are the modal integrals of the girder given by:

$$\Phi = \int_0^L \phi_1^2(x) dx, \quad \Xi = \int_0^L \phi_1(x) \psi_1(x) dx, \quad \text{and} \quad \Psi = \int_0^L \psi_1^2(x) dx \quad (11)$$

and where $L1$ to $L4$ and $M1$ to $M4$ contain the modal integrals of the flaps Φ_f , Ξ_f and Ψ_f , the sum of flutter derivatives referred to the girder and the flaps (see Huynh [1] for full expressions). Finally, note that the flutter mode can be a coupling of more than two modes. In that case, an additional mode gives an additional equation. The determinant condition (8) is still valid, but the calculation of the solution is rather complicated analytically. Generally, the obtained critical wind velocity U_{cr} and the critical frequency ω_{cr} will not be varied by more than 5%, if several similar mode shapes with close frequencies are taken into account in the flutter computation, see Huynh, [1].

9. EXAMPLE

In this section the theory presented above is illustrated by an example taken from Huynh [1]. The suspension bridge shown in figure 15 is considered. It has a streamlined cross-section similar to the cross-section of the Great Belt Bridge. The cable sag is 265 m, the pylon top is 360 m, the girder depth is 4 m, and the girder cross-sectional area is 1.056 m^2 . Applying both FEM and analytical calculation the 1st symmetrical vertical and torsional modes (SV1 and ST1) are 0.404 rad/s and 1.276 rad/s, respectively, see figure 16.

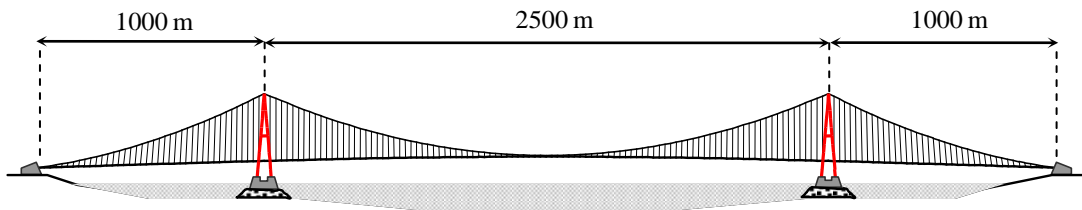


Figure 15: Suspension bridge used in the example.

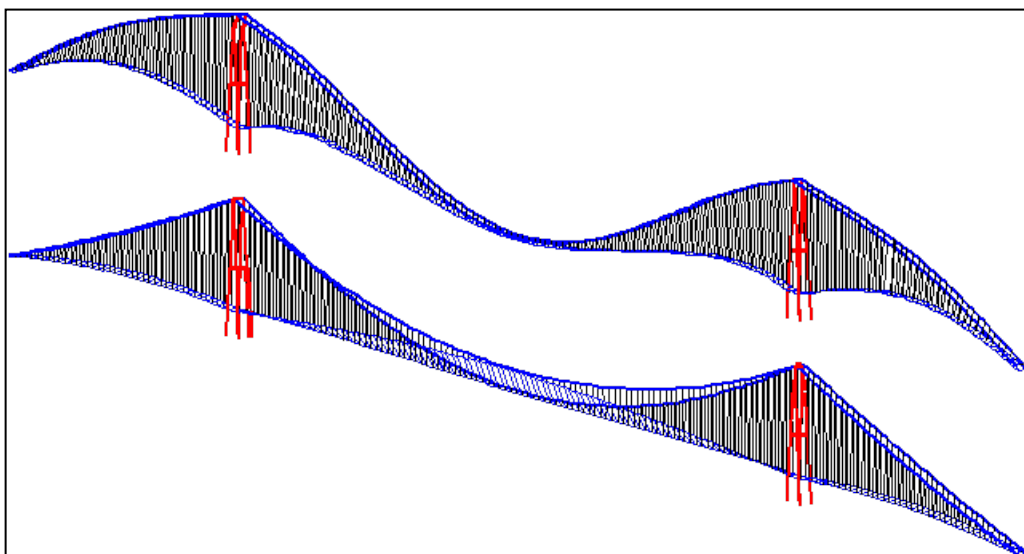


Figure 16. The first symmetrical vertical bending mode (SV1) and the first symmetric torsional mode of the bridge (ST1).

Using flutter conditions similar to (9) and (10), with $F_z^{tot} = F_z^{deck}$ and $F_x^{tot} = F_x^{deck}$, i.e. without flaps, the critical wind velocity is $U_{cr} = 58.21 \text{ m/s}$ and the

corresponding critical frequency is $\omega_{cr} = 0.853$ rad/s. With flaps, the increase of U_{cr} obtained from the conditions (8) and (9) depends on the three flap factors: the lengths (i.e. modal integrals Φ_f , Ξ_f and Ψ_f), the rotational direction (i.e. the signs of r_x^{le} and r_x^{tr} , which are defined positive clockwise) and the rotational magnitudes (in terms of amplification factor a multiplied by the girder rotation r_x , e.g. $r_x^{le}(x,t) = a_{le}r_x(x,t) = a_{le}\alpha(t)\psi(x)$).

The most effective configuration of the flaps against flutter is the configuration Minus + Plus (CMP), where the leading flap rotates against the girder $r_x^{le} = -a_{le}r_x$, and the trailing flap rotates with the girder $r_x^{tr} = a_{tr}r_x$, see figure 16.

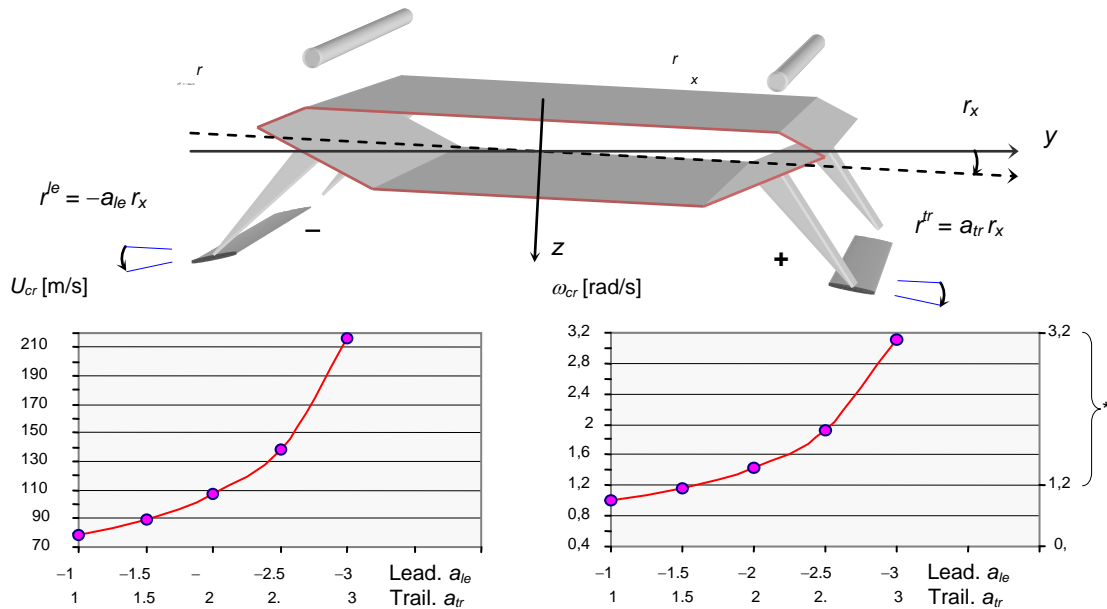


Figure 17: Flutter in CMP with flaps along the whole girder (* ω_{cr} exceeds the ST1 frequency).

Figure 17 shows the increase of U_{cr} and ω_{cr} for increasing a_{le} and a_{tr} . For $r_x^{le} = -1.5r_x$ and $r_x^{tr} = 1.5r_x$, U_{cr} increases from 58.2 to 89.6m/s, i.e. 54%. The critical frequency ω_{cr} increases to the ST1 frequency (the torsional divergent flutter). By increasing a_{le} and a_{tr} up to -3 and 3 , U_{cr} and ω_{cr} can still be found, but ω_{cr} exceeds the ST1 frequency indicating that the higher modes can be involved in the flutter. Therefore, the length of the flaps can be reduced to 46% of the main span length in the centre to obtain an increase of U_{cr} by 50%, and $\omega_{cr} = 1.250$ rad/s.

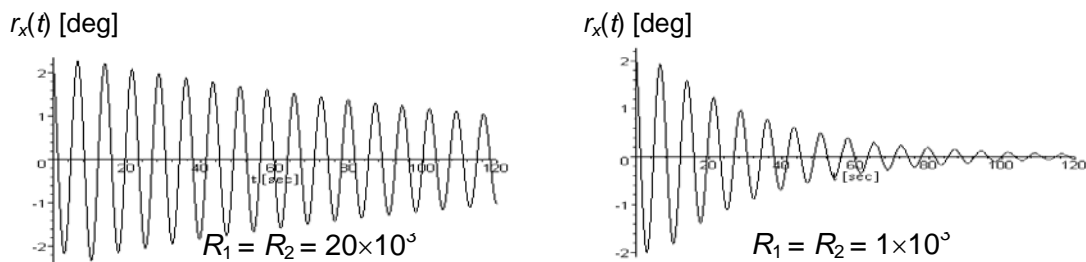


Figure 18: Control of vertical response in the main span centre.

The numerical results of the time history of the control responses and the control forces are shown in figures 18 to 21 with two choices of a control weighting factor R_i in mode I . The reduced control-weighting factor R means that more control forces are required. The state weighting matrix Q has been chosen as the identity matrix, i.e. the vertical and torsional modes are weighted equally. The time history shows the results at the main span centre after the control responses have been multiplied by the mode shape values at mid-span for the vertical and the torsional modes. The maximum vertical response is approximately 0.8 m and the maximum torsional response is about 2 degrees at the centre main span. These magnitudes are damped to zero after approximately two minutes, Huynh [1].

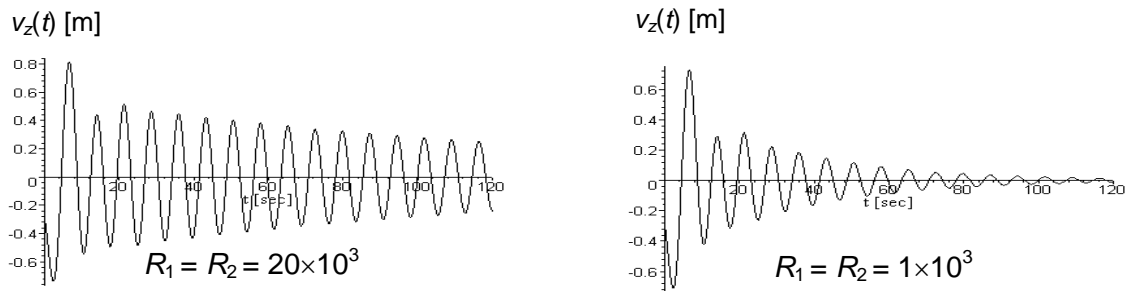


Figure 19: Actual control lift.

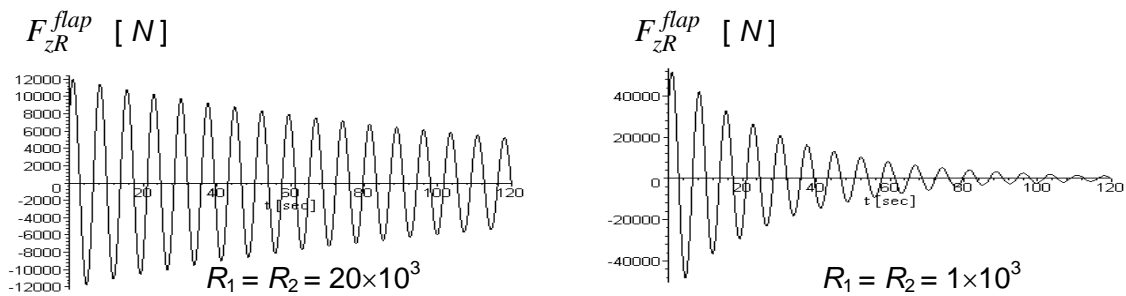


Figure 20: Control of torsional response in the main span centre.

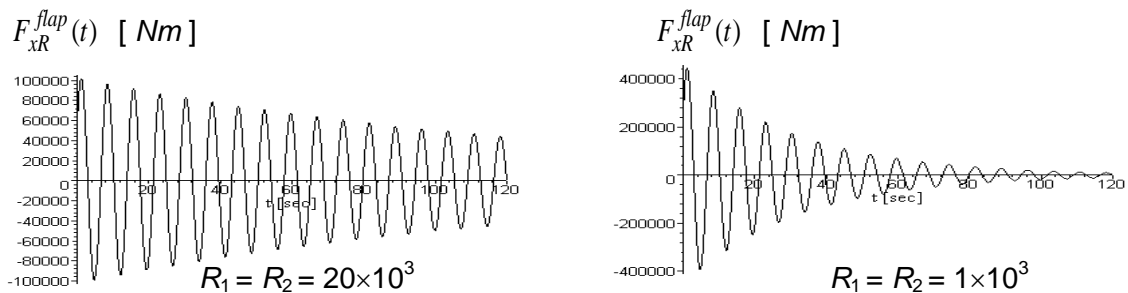


Figure 21: Actual control moment.

10. CONCLUSION

Sectional wind tunnel tests and full bridge computations have shown that the integrated and separate flaps are effective to increase the critical wind velocity of the bridge. It can be shown for the considered example that the flutter velocity U_{cr} can be increased unlimited if the flaps rotate more than three times the girder rotation and if flaps at 46 % of the main span length in the centre of the main span are used. However, the problem with control spillovers needs more investigation, e.g. the computation of different flap configurations acting simultaneously. Further, experiments with full-span bridge with different lengths of the flaps should be performed.

11. REFERENCES

- [1] Huynh, T. Suspension Bridge Aerodynamics and Active Vibration Control. Ph.D. thesis, Aalborg University, Denmark, 2000.
- [2] Ostenfeld, K.H. & A. Larsen. Bridge Engineering and Aerodynamics. In Aerodynamics of Large Bridges (editor A. Larsen), Proc. First Int. Symp. Aerodynamics of Large Bridges, Copenhagen, Denmark, 1992.
- [3] Hansen, H.I. Active Vibration Control of Long Suspension Bridges. Ph.D. thesis, Aalborg University, Denmark, 1998.
- [4] Hansen, H.I. & P. Thoft-Christensen. Wind Tunnel testing of Active Control System for Bridges. Proc. IABSE Congress, Copenhagen, Denmark, 1996, pp.775-780.
- [5] Hansen, H.I. & P. Thoft-Christensen. Active Vibration Control of Long Bridges Using Flaps. Proc. Second World Conf. Struct. Control, Kyoto, Japan, 1998.
- [6] Hansen, H.I. & P. Thoft-Christensen. Wind Tunnel Experiments with Active Control of Bridge Section Model. IABSE Symp. On "Long-Span and High-Rise Structures, Kobe, Japan, 1998, pp.199-204.
- [7] Hansen, H.I. & P. Thoft-Christensen. Active Flap Control of Long Suspension Bridges. Journal of Structural Control, Vol. 8, 2001, pp. 33-82.
- [8] Hansen, H.I., P. Thoft-Christensen, P.A. Mendes & F.A. Branco. Wind Tunnel Tests of a Bridge Model with Active Vibration Control. Structural Engineering International, IABSE, 4/2000, pp.249-253.
- [9] Huynh, T. & P. Thoft-Christensen. Suspension Bridge Flutter for Girders with Separate Control Flaps. Journal of Bridge Engineering, ASCE, Vol. 6, PP. 168-175, 2001.
- [10] Huynh, T. & P. Thoft-Christensen. Buffeting Response of Suspension Bridge Girder with Separate Control Flaps. Second European Conference on Structural Control, Champs-sur-Marne, France, July 3-6, 2000.
- [11] Thoft-Christensen, P. Active Control of Suspension Bridges. Second European Conference on Structural Control, Champs-sur-Marne, France, July 3-6, 2000.
- [12] Theodorsen, T: General Theory of Aerodynamic Instability and the Mechanism of Flutter. NACA Report No. 496, 1935.
- [13] Scanlan, R.H. & J.J.Tomko: Airfoil and Bridge Deck Flutter Derivatives. J.Eng.Mech.Div., ASCE, Paper 8601, 1971, pp. 1717-1737.
- [14] Simiu E. & R.H. Scanlan. Wind Effects on Structures: Fundamentals and Applications to Design, Third Edition, John Wiley and Sons, 1996.
- [15] Meirovitch,L. Dynamics and Control of Structures. John Wiley & Sons, 1990.

